Bifurcation Sequences of a Coulomb Friction Oscillator

B. F. FEENY
ETH Zurich, Institute for Robotics, CH-8092 Zürich, Switzerland

F. C. MOON
Cornell University, Ithaca, New York 14853, U.S.A.

(Received: 18 April 1991; accepted: 12 February 1992)

Abstract. In some parameter ranges, the dynamics of a forced oscillator with Coulomb friction dependent on both displacement and velocity is reducible to the dynamics of a one-dimensional map. In numerical simulations, period-doubling bifurcations are observed for the oscillator. In this bifurcation procedure, the map arising from the Coulomb model may not have 'standard' form. The bifurcation sequence of the Coulomb model is compared to that of the standard one-dimensional maps to see if it exhibits 'universal' behavior. All observed components of the bifurcation sequence fit the universal sequence, although some universal events are not witnessed.

Key words: Bifurcations, chaos, Coulomb friction, universality.

Introduction

The effects of friction in dynamics is potentially important in many areas of modern technology, such as pin-jointed space structures, automobiles, railroads, and robotics. Friction is also important in understanding our own environment, for example in the study of the sliding of tectonic plates. Thus, there is motivation for much research in this area.

As there has been recent interest in strange phenomena, some systems with friction have been shown to exhibit chaos. Grabec [1] modeled chaotic chatter of tool bits using friction and plasticity. Popp and Stelter [2] revealed chaotic behavior in a periodically forced belt-driven mass-spring oscillator, and in a belt-driven continuum. Carlson and Langer [3] studied a mechanical model of an earthquake fault, combining a discretized mass-spring system with a continuous system to yield unpredictable, complicated, catastrophic dynamics.

Our focus is on a harmonically forced single-degree-of-freedom oscillator whose magnitude of friction varies linearly with displacement. A mechanics model is shown in Figure 1. The nondimensional equation of motion is

$$\ddot{x} + 2\zeta\dot{x} + x + n(x)f(\dot{x}) = a\cos\Omega t\,, \tag{1}$$

where $n(x)$ represents the normal load, and ζ is the damping ratio for the oscillator when the friction is removed. The coefficient of friction $f(\dot{x})$ obeys the Coulomb friction law, and hence the following rules:

$$f(\dot{x}) = -\mu_k\,, \quad \dot{x} < 0\,,$$

Nonlinear Dynamics **4**: 25–37, 1993.

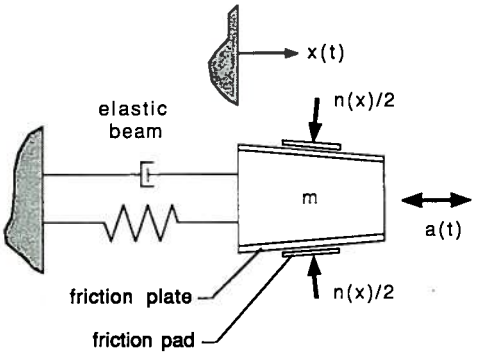

Fig. 1. Mechanics model for a forced oscillator with dry friction. The friction plates are fixed to the mass m, and slide relative to the friction pads, which are fixed in x. The friction surfaces are not paralleled in the direction of displacement x. Thus, the elastically loaded normal forces vary with displacement.

$$-\mu_s \leq f(\dot{x}) \leq \mu_s\,, \quad \dot{x} = 0\,,$$
$$f(\dot{x}) = \mu_k\,, \quad \dot{x} > 0\,, \tag{2}$$

where μ_k is the kinetic friction coefficient, and μ_s is the static friction coefficient. Den Hartog [4] solved the case in which the normal load is constant ($n(x) \equiv 1$ nondimensionally) for periodic motions. Shaw [5] extended Den Hartog's results and included a stability analysis.

Our system differs by allowing $n(x)$ to be nonconstant. We let $n(x) = 1 + kx$ for $x > -1/k$, and $n(x) = 0$ for $x \leq -1/k$ to model a linearly varying normal load which goes to zero when the sliding contact is lost. An oscillator with a somewhat similar friction law has been analyzed by Anderson and Ferri [6]. In particular, we look at the case of $\mu_s = \mu_k = 1$.

The undriven oscillator has a locus of infinitely many equilibria. When excited, oscillators with friction exhibit *stick-slip motion* [4, 5, 7–9]. Sticking occurs when the velocity goes through zero, and the external forces are such that the position is in this locus of equilibria. However, as the magnitude of the periodic driving force increases, it soon reaches a value such that equilibrium can no longer be maintained, and slipping motion resumes.

The oscillator of equation (1) can undergo regular and chaotic dynamics [7, 8]. An example of motion in the state of chaos is shown in Figure 2 as a three-dimensional phase portrait in cylindrical coordinates. In the figure, x is the radial axis, t is the circumferential axis, and $\dot{x}$ is the longitudinal axis. Due to the periodicity of the driver, the x axis can be wrapped around to form the toroidal structure. Sticking motion can be seen as the green, planar portion of the image, confined to zero velocity. Motion with positive velocity is shown in white, and motion with negative velocity is shown in yellow. A trajectory starting near the outside edge of this deformed torus evolves clockwise in time, returning near the outside edge after one revolution around the torus. A trajectory starting near the inside, however, goes through the loop in positive velocity and returns near the outside edge of the torus. The orbits in between are stretched and folded during this action. This stretching and folding is the mechanism of chaos.

A Poincaré section, viewed as a slice in the time axis, is shown in Figure 3a. On a large portion of this image, $\dot{x} = 0$, and the motion is sticking. On the rest of the image, $\dot{x} > 0$, and the motion is slipping. Performing a return map on a coordinate s defined along the Poincaré section reveals a one-dimensional single-humped map $F(s)$ (Figure 3b). Thus, a one-dimensional map underlies the dynamics of the oscillator. This is also true in the corresponding experimental system

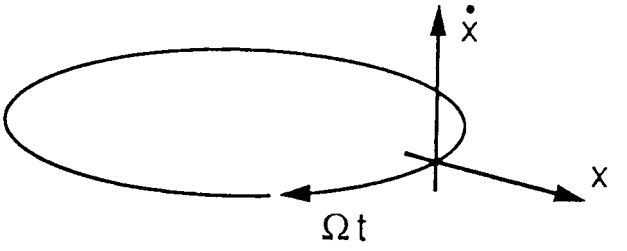

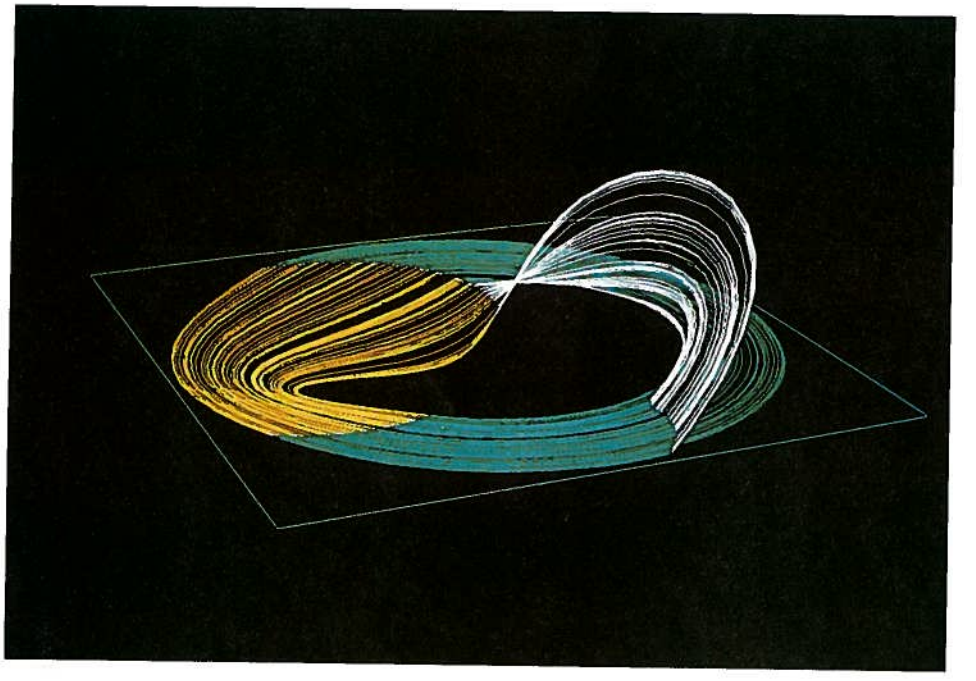

Fig. 2. Numerical solution for equation (1) with $\zeta = 0$, $a = 1.9$, $\Omega = 1.25$, and $k = 1.5$. Viewed in cylindrical coordinates, the displacement is the radial axis, velocity is the longitudinal axis, and time is the circumferential axis. Green indicates orbits in sticking motion, white represents orbits with positive velocity, and yellow depicts motion with negative velocity.

[7, 8]. We will describe how the one-dimensional map arises in the Coulomb model in a later section.

Period doubling is the observed route to chaos. Figure 4 depicts the bifurcation diagram with increasing parameter a.

Stick-slip motion provides a natural basis for producing symbol sequences during the motion, where, for example, S represents motion which is sticking, and N represents motion which is not sticking (slipping). For an experimental oscillator and a similar model, we had previously exploited binary symbol dynamics to characterize chaos using binary autocorrelation functions and macroscopic Lyapunov exponents [10].

In this paper, we extend the study by comparing the bifurcation sequence, and its associated symbol sequences, of the Coulomb oscillator, with the 'universal' bifurcation sequence of 'standard' one-dimensional maps. Universal behavior refers to behavior that is consistent for all parameter ranges in a given class of systems [11].

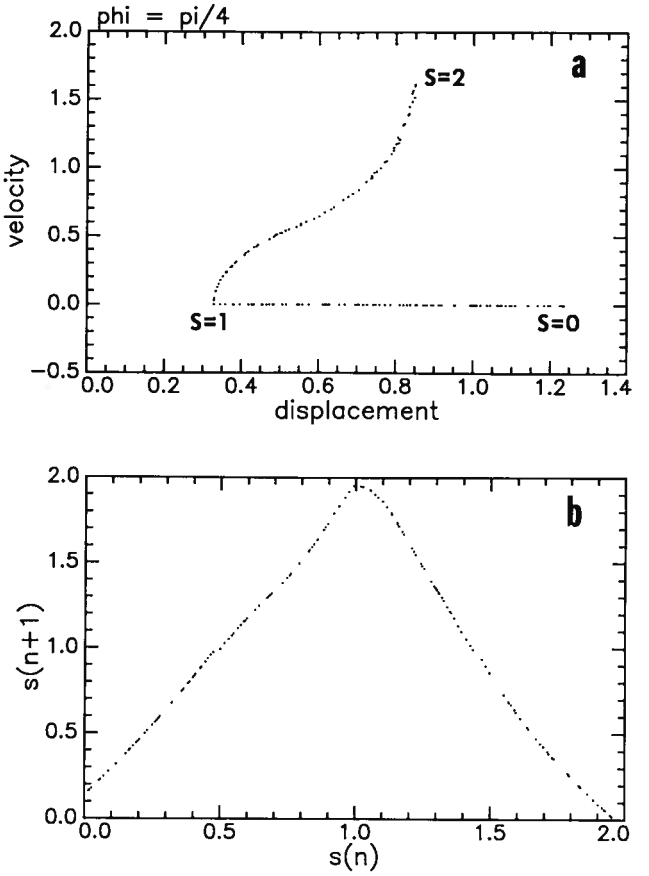

Fig. 3(a). A Poincaré section of the numerical solution in Figure 2. (b) A return map on a coordinate s defined along the Poincaré section reveals the underlying one-dimensional map $F(s)$.

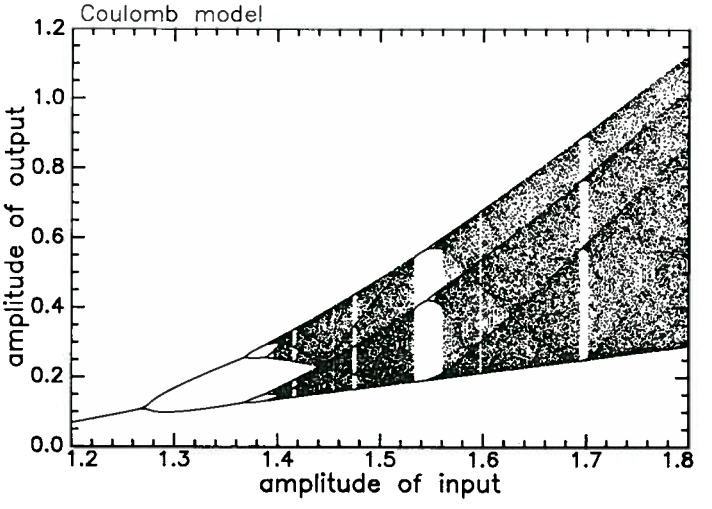

Fig. 4. A bifurcation diagram shows period doubling to be the route to chaos. The bifurcation parameter, the driving amplitude a, is increasing in this plot.

From a mathematical viewpoint, universal behavior of standard maps has been studied in detail. Thus, if a dynamical system exhibits universal behavior, then much is already known about the system. In terms of system identification, examining whether behavior is universal might give a clue as to whether the unknown system fits a standard class of systems. On the other hand, for parametric system identification, where differences in behavior with respect to system parameters is of importance, interest might be focused on nonuniform behavior.

Bifurcations of One-Dimensional Maps

One-dimensional maps of the type

$$x_{n+1} = \lambda g(x_n)\,, \tag{3}$$

where the function $g(x)$ satisfies certain assumptions, have been studied extensively [11–14]. When considering universal sequences of periodic orbits, the critical assumptions are that

1. $g(0) = g(1) = 0$,
2. $g(x)$ is smooth with a unique maximum at x_0, and $\lambda > 0$, and
3. $g(x)$ has a negative Schwartzian derivative for $x \in [0, 1] - \{x_0\}$,

where the Schwartzian derivative for a function $g(x)$ is defined as

$$D_s g(x) = \frac{g'''(x)}{g'(x)} - \frac{3}{2}\left(\frac{g''(x)}{g'(x)}\right)^2 .$$

For discussions on metric universality, i.e., Feigenbaum numbers, we can relax the above assumptions, and only assume $g''(x_0) < 0$.

The dynamics of maps which satisfy assumptions 1 through 3 undergo a universal sequence of bifurcations, where the bifurcation parameter is λ. For $\lambda = \lambda_1$ sufficiently small, such that $\bar{x} = \lambda_1 g(\bar{x})$, and $|\lambda_1 g'(\bar{x})| < 1$, $\bar{x}$ is a stable periodic point of $\lambda g(x)$. As λ increases, a periodic cycle remains until $\lambda = \lambda_2$, at which the periodic point loses stability and a stable periodic cycle of period two is born. A stable cycle of period two exists until $\lambda = \lambda_4$, where the period two loses stability and a period four is born. This period-doubling sequence continues, producing stable periodic cycles of period 2^n, $n \to \infty$, as λ approaches a limiting value λ_∞. Given any λ such that $\lambda_\infty < \lambda < \lambda_c$, there exists an infinite number of unstable periodic cycles and a stable cycle of period n. The stable cycle undergoes a similar period-doubling sequence as above, to a limiting value of $\lambda_{n\infty}$. Typically, on a bifurcation diagram, windows of relatively low period n are identifiable to the eye. When $\lambda > \lambda_c$, orbits become unbounded.

The bifurcation sequence of the map (3) exhibits universal behavior, that is behavior common to any function $g(x)$ which satisfies the assumptions stated above. As the bifurcation parameter increases, there will be a bifurcation sequence of stable periodic orbits. From this sequence, we could construct a sequence of the period lengths of these stable cycles. A universal property is that this sequence of period lengths is the same for all such maps. For each stable periodic cycle, there exists a parameter value $\hat{\lambda}$ such that one point p_0 of the periodic sequence lies at x_0. The value of a periodic point $p_0(\lambda)$ is continuous in λ, and there is a region $(\hat{\lambda} - \delta_1, \hat{\lambda} + \delta_2)$, for some $\delta_1 > 0$, $\delta_2 > 0$, such that the periodic cycle remains stable, and p_0 stays near x_0 [13].

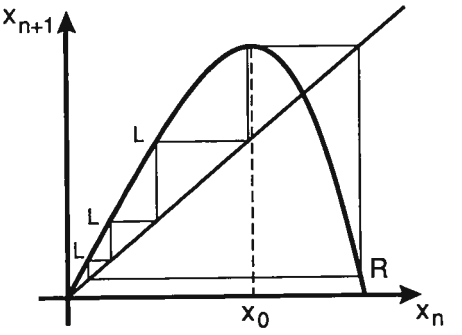

Fig. 5. A periodic cycle of period five for a one-dimensional map. Points to the right of x_0 are labeled R, and points to the left of x_0 are labeled L. The symbol sequence RLLL refers to the four iterates of the periodic-cycle point (period five) nearest x_0.

A symbol sequence for the periodic cycle can be defined by whether the ith iterate in the cycle is to the right of $x_0(R)$ or to the left of $x_0(L)$. Since p_0 is arbitrarily close to x_0, we assign the symbol C to p_0. For a cycle of period m, the remaining $m-1$ iterates of p_0 are assigned the symbols R and L. For example, if the periodic cycle had a period of five, the symbol sequence might be CRLLL, pertaining to iterates of the point located very near x_0. The convention in the literature [13, 14] is to drop the symbol C. Therefore, a symbol sequence for a periodic cycle of period m is defined as the symbols of the $m-1$ iterates of p_0. In our example, the period-five symbol sequence is defined by the four symbols RLLL. This example is illustrated in Figure 5. A second universal property is that the symbol sequences of each of these stable periodic orbits is the same for all such maps.

Metric universality exists for maps which merely satisfy $g''(x_0)<0$. In this case, the period-doubling sequence occurs according to Feigenbaum's ratio [11, 12]. If λ_n is the parameter value for a cycle of period $m2^n$, then Feigenbaum's ratio is

$$\delta = \lim_{n\to\infty} \frac{\lambda_{n+1} - \lambda_n}{\lambda_{n+2} - \lambda_{n+21}} = 4.6692\ldots.$$

On the Coulomb Oscillator

The purpose of this section is to provide some background on the Coulomb oscillator, and to demonstrate the source of the underlying one-dimensional map. Further details can be found in references [7, 9].

System Geometry

A geometrical description of the dynamics of the friction oscillator can be used to explain the source of the one-dimensional map $F(s)$, and also to indicate the difficulty involved in obtaining an analytical expression for the map. Some interesting dynamical properties resulting from the one-dimensional map are also noted.

The discontinuity at $\dot{x}=0$ is a convenient location for defining a map. In state space, the plane D of discontinuity is the (x, t) plane at $\dot{x}=0$. The plane D separates two regions in which

the governing equations of motion are smooth. For $\dot{x} > 0$, the system ($\zeta = 0$) obeys

$$\ddot{x} + (1 + k)x = -1 + a\cos(\Omega t)\,, \tag{4}$$

while for $\dot{x} < 0$, the system follows

$$\ddot{x} + (1 - k)x = 1 + a\cos(\Omega t)\,. \tag{5}$$

We examine the system when $k > 1$. In this case, when undriven, equation (4) contains a center, and equation (5) has a saddle point.

Sticking regions can be described by observing the directions of the piecewise continuous vector fields at D. When both vector fields agree to flow through D, the flow may pass through the discontinuity. When both vector fields point toward D, there is a stable sticking region R. Flows are trapped in R until time evolves such that the orbits are on either of the boundaries, B^+ or B^-, of the sticking region. A map describing this action would be $S : R \to B^+ \cup B^-$. S is singular since it takes a two-dimensional region R and maps it into a finite union of curves. Figure 6 shows the sticking regions for our system. $\oplus$ indicates the region where both vector fields at D point towards positive velocity, and $\ominus$ depicts the regions where both vector fields point towards negative velocity.

The map corresponding to the flow of equation (4) can be written as $P^+ : \oplus \to R \cup \ominus$. The map corresponding to the flow of equation (5) can be written as $P^- \ominus : R \cup \oplus$. The dynamics can be described in terms of these maps on D in the variables x and t, in conjunction with the map S.

Figure 7 shows the evolution of the entire set of orbits passing through $\ominus$ for $a = 1.9$, $\Omega = 1.5$, and $k = 1.5$. For these parameters, the entire two-dimensional region $\ominus$ collapses into a one-dimensional curve. This geometrically illustrates the singularity which produces the one-dimensional map $F(s)$. The singularity is in the mapping S in the sticking region.

In this example, all motions pass through the sticking region. A sufficient condition which ensures sticking motion is as follows: if $P^-(\ominus) \cap P^{+^{-1}}(\ominus) = \emptyset$, then all motions must pass through the sticking region. Indeed, a numerical test (not presented here) has shown that $P^-(\ominus) \cap P^{+^{-1}}(\ominus) = \emptyset$. For other parameter values, however, it may be that not all motions pass through the sticking region. In such case, a one-dimensional map would not characterize the entire limit set.

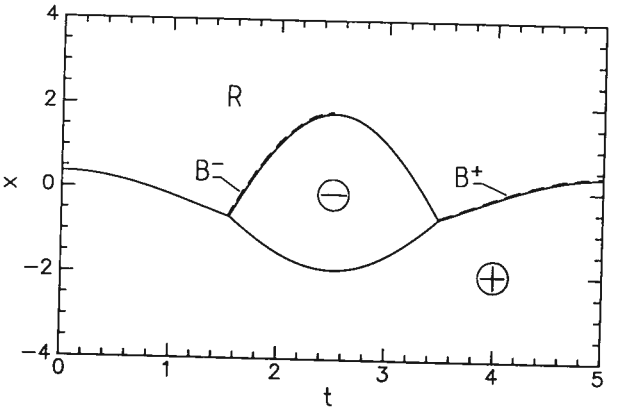

Fig. 6. The sticking region R is depicted in the (x, y) plane D for $k > 1$. The region of flow toward $\dot{x} > 0$ is labeled $\oplus$. The region of flow toward $\dot{x} < 0$ is labeled $\ominus$.

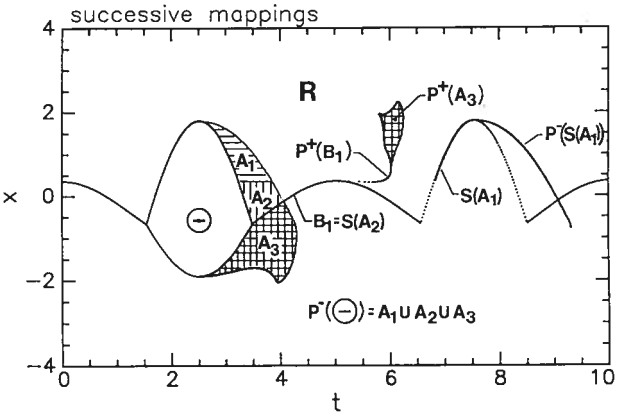

Fig. 7. Successive mappings of $\ominus$ show that, within one period of excitation, the entire set of points has condensed to a line. This is how the one-dimensional map arises. The parameter values are $a = 1.9$, $\Omega = 1.25$, and $k = 1.5$.

When all motions pass through R, knowledge of the mappings of the boundaries B^+ and B^- is sufficient to understand the attracting set.

From the geometric description presented here, certain properties of motion are evident in Figure 7: the attractor has a capacity dimension $d_c \leq 2$; orbits reach the attractor in finite time; and orbits are not invertible, indicating a loss of information regarding the history of motion.

These properties do not occur in smooth vector fields. They result from the dimensional collapse which takes place in sticking motions. Dimensional collapse has been noticed in other contact problems [15] and the properties mentioned can be observed in constrained systems [16]. Finite attraction time and loss of history in non-Lipschitz systems have been discussed by Zak [17], who dubs such attractors 'terminal'.

Dimensional collapse has a profound effect on the topology of the dynamics, and may disrupt analyses (such as embeddings, and calculations of Lyapunov exponents and correlation dimension) traditionally used with smooth systems. There is also a potential for having nonuniform topological descriptions of motion [7].

The Underlying One-Dimensional Map

An analytical expression for $F(s)$ would consist of three components. One component would involve orbits passing through the boundary B^- and their intersection with the plane D, represented by $P^-(B^-)$. Finding $y = P^-(x)$ requires the solution of transcendental equations. The mapping $P^-(B^-)$ lies partly in R and partly in $\oplus$. Thus, the second component of the analytical expression of the one-dimensional map would be a logical operation. The third component would then be to either solve for the time at which trajectories in R leave the sticking region at B^+ or B^-, or else to solve the transcendental equation representing those orbits which map to D via P^+.

In short, the analytical description of $F(s)$ is compounded with transcendental equations and logical operations. Because of this complexity, we do not produce such an analytical expression, and our work is done from a geometric standpoint.

The map $F(s)$ (Figure 3b) may not satisfy all the assumptions in the above discussions. Perhaps most importantly, $F(s)$ does not fit the form of equation (3). It can be shown, for

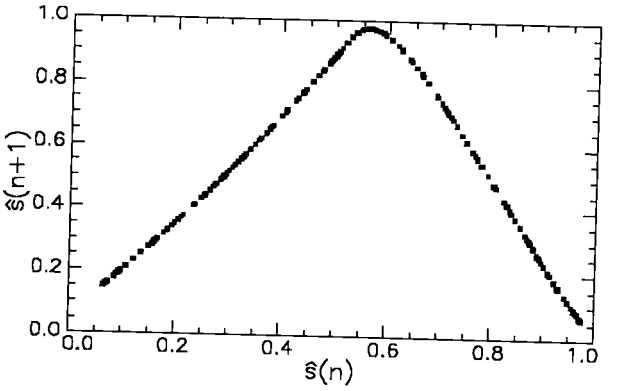

Fig. 8. A return map from a Poincaré section lying entirely in sticking motion reveals evidence that the maximum in the one-dimensional map is smooth of the case of $a = 1.9$, $\Omega = 1.25$, and $k = 1.5$.

example, that as $a \to \infty$, the map $F(s)$, where $s \in I$ is a normalized coordinate, approaches a limit function in both magnitude and shape. Thus, $F(s) \neq ag(s)$.

The 'instantaneous' shape function g satisfies the first assumption (if the coordinate s is rescaled), but not necessarily the third. We do not obtain an explicit expression for the map, and hence do not check its Schwartzian derivative. However, the maximum is smooth, at least for some values of a. This is discussed below. Visual evidence is in Figure 8, which shows a delay map from a Poincaré section taken at a time in which all motions are in the sticking region. Hence, the Poincaré image is straight line and the coordinate $\hat{s}$ is cleanly defined.

To discuss the maximum of $F(s)$, we must first locate it. To this end, we look at the image $P^+(B_1)$ in Figure 7. Close inspection indicates that this image has a local minimum in x at $x = z$ for some value of t_0 ($t_0 \approx 5.5$ in the figure). Additionally, for the given parameters, this point z denotes the maximum value of s in some Poincaré sections. In the Poincaré section at $t = 6.5$, for example, defining a coordinate $\hat{s}$ such that $0 \leq \hat{s} \leq 1$ and $\hat{s} = 1$ at z shows that the point $(z, t = 6.5) \in D$ corresponds to the maximum value of $\hat{s}$. In a Poincaré section at $t = t_0$, the point $(z, t_0) \in D$ represents s_0, locating the local maximum in the underlying map.

Since a small neighborhood $V \in B_1$ of the orbit passing through this critical point is governed solely by a function $P^+(V)$ which maps a curve monotonely increasing in x to a curve with a smooth minimum in x (at $x = z$), the point s_0 represents a smooth maximum in the underlying map.

We should point out that if $P^+(B_1)$ were to lack a local minimum in x, then the point s_0 would correspond to sticking orbits passing through the local maximum of the curve B^+ (Figure 6), and thus s_0 would represent a boundary between two functions active in the one-dimensional map (involving P^+ and P^-). In general, such a map would not have a smooth maximum.

Bifurcation Analysis for the Coulomb Oscillator

The Coulomb oscillator is defined by equations (1) and (2). It is numerically integrated according to an algorithm which accounts for the discontinuity at $\dot{x} = 0$ [2, 7, 8].

Since the equation of motion has a discontinuity at $\dot{x} = 0$, the plane in $(x, \dot{x}, t)$-space defined by $\dot{x} = 0$ is a natural place to make a Poincaré section. In this Poincaré section we plot x for the bifurcation diagram shown in Figure 4. The bifurcation diagram includes trajectories which bounce off the underside ($\dot{x} < 0$) of the (x, t) plane. (Some trajectories meet the (x, t) plane from below, stick, and then return below the plane. This corresponds, for example, to motion near the outer edge of the attractor in Figure 2.)

The method used to compare the bifurcation sequence in the Coulomb friction model to the standard one-dimensional maps is as follows: We compute and plot a bifurcation diagram, which has periodic windows. We identify periodic orbits visible to a parameter increment Δa of $\Delta a + 0.0005$. In doing so, we look for stable periodic orbits of period less than eight. The infinitely many higher periods are difficult to find because the ranges of λ on which they exist are narrow. We compare the sequence of period lengths of stable periodic cycles found in the Coulomb oscillator with the universal sequence of stable periodic cycles. If a period five, say, appears in the bifurcation diagram for a parameter value $a = \hat{a}$, then we observe the Poincaré section (from a slice in time) of the motion with the parameter set to $\hat{a}$. In the Poincaré section the orbit will consist of five points. From this Poincaré section, we can determine the symbol sequence of the periodic points in terms of the sticking and slipping regions. We assign the symbol S to points which are *sticking*, and the symbol N to points which are *not sticking* (slipping). We also compare the symbol sequence of the stable periodic cycles found in the Coulomb oscillator with the universal symbol sequences of stable periodic cycles. Finally, we estimate Feigenbaum numbers from the Coulomb oscillator data.

This sequence of N's and S's will be analogous to the symbol sequence for the associated map, and can be translated into a sequence of R's and L's, respectively. This translation is exact when the Poincaré section is taken at $t \bmod 2\pi/\Omega$ corresponding to t_0. This is because the maximum of the underlying map occurs at the critical point s_0 corresponding to z, which is the local minimum (in x) of curve $P^+(B_1)$. At a phase corresponding to t_0, this point cleanly separates sticking motions from slipping motions, as well as left from right.

However, when $t \neq t_0$, some other value of $s \neq s_0$ separates points that are sticking from points that are slipping. As an extreme case, when $t = 6.5$ in Figure 7, all points are in the sticking region (a symbol sequence would trivially consist only of S's). In the neighborhood of t_0, the approximation of the N's and S's as R's and L's is reasonable due to the smoothness of the curve $P^+(B_1)$. Deviation of the N's and S's from the R's and L's represents an error in observation of behavior, rather than an effect on universality. Our Poincaré section was taken at $t \bmod 2\pi/\Omega \approx 0.625$. Based on Figure 7 viewed at $t \approx 5.6$, error in the symbol dynamics should be small.

Results

A comparison of the sequence of periodic orbits, and their symbol sequences, for the friction oscillator and the logistic map is in Table I. For the logistic map, $x_{n+1} = \lambda g(x_n)$ with $g(x) = x(1 - x)$. The values for the logistic map were obtained from [13] and [14] for periodic orbits of period seven or less. Two higher-period events were added since they were accidentally found in the friction oscillator.

The bifurcation sequence of a Coulomb friction oscillator, in some sense, resembles the universal sequence of standard one-dimensional maps. The observed periodic orbits, their period lengths and symbol sequences, of the Coulomb friction oscillator lie in the sequence of the

TABLE I.

The observed sequence of period length of stable periodic cycles in the Coulomb oscillator, and their symbol sequences, are compared to the sequence of stable periodic cycles in the logistic map. Each cycle listed is the first of an infinite period-doubling sequence, except those marked with a *, which arise from the previous cycle via period doubling.

For the Coulomb oscillator, S indicates points which are sticking, and N indicates points which are not sticking. The symbol • represents a point which was so close to the boundary between N and S that it was not distinguishable.

Each periodic cycle has one point which is very close to this boundary. We label such points with the symbol C. The listed symbol sequence of a cycle of period m consists of the $m-1$ iterates of the point labeled C.

Only cycles up to period seven are included in the table. Some of these cycles in the Coulomb oscillator were not found. Incidents of a period eight and a period ten were accidentally found and included.

Oscillator	Eq. (1)		Map cf. [12, 13]	$x_{n+1} = \lambda x(1-x)$	
Period	Symbol Seq.	a	Period	Symbol Seq.	λ
2	N	1.36	2	R	3.2360680
4*	NSN	1.38	4*	RLR	3.4985167
8*	NSNNNSN	1.3925	8*	RLRRRLR	not listed
10	NSNNNSNSN	1.4064	10	RLRRRLRLR	not listed
6	NSNNN	1.415	6	RLRRR	3.6275575
7	NSNNNN	1.45415	7	RLRRRR	3.7017692
5	NSNN	1.4737	5	RLRR	3.7389149
7	NSNNSN	1.4909	7	RLRRLR	3.7742142
3	NS	1.535	3	RL	3.8318741
6*	NS•NS	1.551	6*	RLLRL	3.8445688
			7	RLLRLR	3.8860459
5	NSSN	1.5973	5	RLLR	3.9057065
			7	RLLRRR	3.9221934
			6	RLLRR	3.9375364
			7	RLLRRL	3.9510322
4	NSS	1.695	4	RLL	3.9602701
			7	RLLLRL	3.9689769
			6	RLLLR	3.9777664
			7	RLLLRR	3.9847476
5	NSSS	1.833	5	RLLL	3.9902670
			7	RLLLLR	3.9945378
			6	RLLLL	3.9975831
			7	RLLLLL	3.9993971

standard maps, although several events remain undetected. In other words, every event in the oscillator is also in the universal sequence of events (but not *vice versa*), and the order of events in the oscillator does not contradict the order in the universal sequence. Furthermore, the symbol sequences associated with each observed periodic cycle in the Coulomb friction oscillator is the same as in the corresponding periodic cycle in the standard one-dimensional maps.

There are two possible explanations for the fact that some bifurcation events were not detected. One possibility is that these events took place on a parameter window smaller than the resolution at which we chose to search. The other possibility is that the bifurcation sequence of the oscillator in fact may not match the universal sequence of the standard maps. Such deviation could occur since the map which arises from the Coulomb oscillator may not satisfy all of the assumptions required for universal behavior in the standard maps. Thus, it is possible that we are observing a nonuniversal bifurcation sequence in the Coulomb oscillator. Coffman *et al.* [18] previously observed nonuniversal behaviour in nonstandard one-dimensional maps. In that study, the nonuniversal events also occured in the universal sequence, but not according to the universal order.

In the investigation of metric universality, the parameter values in the initial period-doubling sequence were measured to be compared with Feigenbaum's ratio. We measured the parameter value a_2 at the first period-doubling bifurcation, and a_4, a_8, and a_{16} at the subsequent bifurcations. We then compared

$$r_1 = \frac{a_4 - a_2}{a_8 - a_4}$$

and

$$r_2 = \frac{a_8 - a_4}{a_{16} - a_8}$$

to Feigenbaum's ratio of 4.669 . . . . The estimates are $r_1 = 4.70 \pm 0.25$ and $r_2 = 4.67 \pm 0.65$. In the estimates, the parameter increment was smaller than that of the rest of this investigation. The uncertainty is in the numerical integration. Within the scope of the error, it would not be unusual for the ratio to converge nonuniformly. Higher bifurcations involve smaller window sizes, leading to larger errors in the calculations of the r_i.

Conclusions

The dynamics of the Coulomb friction oscillator is reducible to the dynamics of a non-invertible one-dimensional map. The map is not proportional to the bifurcation parameter. Because of this, and because of other considerations, such as the Schwartzian derivative, the map may not fit the description of the 'standard' maps. Nonetheless, the bifurcation sequence of the oscillator has been compared to that of the standard one-dimensional maps.

The observed periodic orbits, their period lengths and symbol sequences, fit into the universal sequence. However, several universal events remain undetected. This may be because the necessary assumptions are not all met, and that the oscillator does indeed exhibit nonuniversal behavior. However, consideration must be given to the size of the increment in the bifurcation parameter, Δa. If a periodic window is smaller than Δa, the window may not be observed. Therefore, a statement regarding the nonexistence of a periodic window cannot be made, since Δa can always be made smaller.

Acknowledgements

We are grateful to Professor Philip Holmes for his helpful comments and suggestions. We also thank Bill Holmes for maintaining the computer cluster, and Bill Feeny for assisting in the graphics. This work was supported by grants from IBM, the ARO, and the AFOSR.

References

1. Grabec, I., 'Chaos generated by the cutting process', *Physics Letters A* **117** (8), 1986, 384–386.
2. Popp, K. and Stelter, P., 'Nonlinear oscillations of structures induced by dry friction', in W. Schiehlen (ed.), *Nonlinear Dynamics in Engineering Systems*, Berlin-Heidelberg: Springer-Verlag, 1990.

3. Carlson, J. M. and Langer, J. S., 'Mechanical model of an earthquake fault', *Physical Review A* **40**(11), 1989, 6470–6484.
4. Den Hartog, J. P., 'Forced vibrations with combined Coulomb and viscous friction', *Transactions of the ASME* **53**, 1931, 107–115.
5. Shaw, S. W., 'On the dynamic response of a system with dry friction', *Journal of Sound and Vibration* **108**(2), 1986, 305–325.
6. Anderson, J. R. and Ferri, A. A., 'Behavior of a single-degree-of-freedom system with a generalized friction law', *Journal of Sound and Vibration* **140**(2), 1990, 287–304.
7. Feeny, B., 'Chaos and Friction', PhD Thesis, Theoretical and Applied Mechanics, Cornell University, 1990.
8. Feeny, B. and Moon, F. C., 'Chaos in a dry-friction oscillator: experiment and numerical modeling', submitted to the *Journal of Sound and Vibration*.
9. Feeny, B., 'A nonsmooth Coulomb friction oscillator', to appear in *Physica D*.
10. Feeny, B. F. and Moon, F. C., 'Autocorrelation on symbol dynamics for a chaotic dry-friction oscillator', *Physics Letters A* **141**(8, 9), 1989, 397–400.
11. Devaney, R. L., *An Introduction to Chaotic Dynamical Systems*, Addison–Wesley, Redwood City, California, 1987.
12. Feigenbaum, M. J., 'Quantitative universality for a class of nonlinear transformations', *Journal of Statistical Physics* **19**(1), 1978, 25–52.
13. Metropolis, N., Stein, M. L., and Stein, P. R., 'On finite limit sets for transformations on the unit interval', *Journal of Combinatorial Theory* **15**(1), 1973, 25–44.
14. Schuster, H. G., *Deterministic Chaos: an Introduction*, VCH Publishers, Weinheim, Federal Republic of Germany, 1988.
15. Szczygielski, W. and Schweitzer, G., 'Dynamics of a high-speed rotor touching a boundary', in G. Bianchi and W. Schiehlen (eds.), *Dynamics of Multibody Systems*, IUTAM/IFToMM Symposium Udine 1985, Springer, Berlin Heidelberg 1986, 287–298.
16. Oka, H. and Kokubu, H., 'An approach to constrained equations and strange attractors', *Patterns and Waves – Qualitative Analysis of Nonlinear Differential Equations*, 1986, 607–630.
17. Zak, Michail, 'Terminal attractors in neural networks', *Neural Networks* **2**, 1989, 259–274.
18. Coffman, K., McCormick, W. D., and Swinney, L., 'Multiplicity in a chemical reaction with one-dimensional dynamics', *Physical Review Letters* **56**(10), 1986, 999–1002.